
MACHINE LEARNING BASED DIGITAL TWIN FOR STOCHASTIC NONLINEAR MULTI-DEGREE OF FREEDOM DYNAMICAL SYSTEM

A PREPRINT

Shailesh Garg

Department of Civil Engineering
Indian Institute of Technology Guwahati
Guwahati, Assam 781039, India.
shailesh.garg@iitg.ac.in

Ankush Gogoi

Department of Civil Engineering
Indian Institute of Technology Guwahati
Guwahati, Assam 781039, India.
ankushgogoi1@gmail.com

Souvik Chakraborty

Department of Applied Mechanics
Indian Institute of Technology Delhi
Hauz Khas, New Delhi 110016, India.
souvik@am.iitd.ac.in

Budhaditya Hazra

Department of Civil Engineering
Indian Institute of Technology Guwahati
Guwahati, Assam 781039, India.
budhaditya.hazra@iitg.ac.in

January 6, 2022

ABSTRACT

The potential of digital twin technology is immense, specifically in the infrastructure, aerospace, and automotive sector. However, practical implementation of this technology is not at an expected speed, specifically because of lack of application-specific details. In this paper, we propose a novel digital twin framework for stochastic nonlinear multi-degree of freedom (MDOF) dynamical systems. The approach proposed in this paper strategically decouples the problem into two time-scales – (a) a fast time-scale governing the system dynamics and (b) a slow time-scale governing the degradation in the system. The proposed digital twin has four components - (a) a physics-based nominal model (low-fidelity), (b) a Bayesian filtering algorithm a (c) a supervised machine learning algorithm and (d) a high-fidelity model for predicting future responses. The physics-based nominal model combined with Bayesian filtering is used for combined parameter state estimation and the supervised machine learning algorithm is used for learning the temporal evolution of the parameters. While the proposed framework can be used with any choice of Bayesian filtering and machine learning algorithm, we propose to use unscented Kalman filter and Gaussian process. Performance of the proposed approach is illustrated using two examples. Results obtained indicate the applicability and excellent performance of the proposed digital twin framework.

Keywords Digital Twin · Bayesian Filters · Gaussian process · Non-linear MDOF Systems

1 Introduction

A digital twin (DT) is a digital/virtual representation of a physical system, often referred to as the physical twin. The virtual model resides in the cloud and is connected to the physical counterpart through internet of things (IoT) [1]; the key premise here is to achieve temporal synchronization between the physical and digital twins. This necessitates continuous updation of the DT based on sensor data. It may be noted that the DT can also actuate the physical counterpart through actuators. Once a DT is in sync with the physical counterpart, it can be used to do a number of tasks including decision making [2], remaining useful-life estimation [3] and preventive maintenance optimization [4]. The possibilities offered by the DT technology are immense, evident from the recent applications of this technology in prognostics and health monitoring [5, 6], manufacturing [7, 8], automotive and aerospace engineering [9, 10], to mention a few. In this paper, the primary objective is the development of a DT for nonlinear dynamical systems.

Developing DTs for dynamical systems is challenging because of the presence of, at least, two different time-scales. The responses of dynamical systems are governed by external excitations and their fluctuations thereof; and typically encode the characteristic time period of a system. On the other hand, the operational life of a dynamical system is rather large. To put things into perspective, for example, consider a wind turbine, where the characteristic time period is of the order of tens (10s) of seconds [11] while the operational life is in tens of years. Incorporating this fundamental mismatch within a DT is non-trivial. In [12], a digital twin framework for dynamical systems that decouples the two timescales was presented. Simple analytical formulae for capturing variation of mass and stiffness with operational time-period were proposed. The framework was later extended in [13] wherein, a Gaussian Process (GP) [14, 15, 16] was employed for tracking the time evolution of the system parameters. However, both these frameworks are only applicable when the underlying system is of linear single-degree-of-freedom type. In practice, most real-life dynamical systems are nonlinear with multiple degrees-of-freedom [17, 18]. DT for multi-timescale dynamical systems [19] and bars [20] can also be found in literature.

From the discussion above, it is evident that the literature on DT for dynamical systems is quite sparse. In fact, to the best of the knowledge of the authors, there exists no work on digital twin for nonlinear MDOF dynamical systems. In order to fill this apparent void, a novel algorithm for building DT of stochastic nonlinear MDOF dynamical systems is proposed. Following [12], the proposed framework also decouples the fast and the slow-timescales. We propose to use nonlinear Bayesian filters [21, 22, 23] and machine learning [24, 25, 26, 27, 28, 29] for estimating the system parameters in the fast and slow timescales, respectively. It may be noted that the use of Bayesian filters is already quite prevalent for state and parameter estimation. Works carried out in [15, 30, 31, 32, 33] illustrate use of Bayesian filters for state and parameter estimation of linear/non-linear MDOF systems subjected to deterministic loading; however, such filters are only effective over a short time-scale (a few seconds). The objective here is to develop a DT that can operate over the operational life of a system and hence, directly usage of a Bayesian filter is not an option. This motivates the coupling Bayesian filter with an appropriate machine learning algorithm. Among different Bayesian filtering algorithms present in literature, we propose to use unscented Kalman Filter (UKF) [34]. On the other hand, among different machine learning algorithms existing in the literature, Gaussian process (GP) [15, 16, 28, 29] is used as the machine learning algorithm. The advantage of GP resides in the fact that it is a probabilistic machine learning algorithm and hence, immune from overfitting. Additionally, it also provides a confidence interval, which is useful in the decision making process. However, one must note that the proposed approach is generic in nature and can be used with any choice of Bayesian filtering and ML algorithms.

The rest of the paper is organized as follows. The dynamic model for the digital twin of nonlinear dynamical systems is discussed in Section 2. The problem statement is also stated clearly in this section. UKF and GP are briefly discussed in Sections 3 and 4 respectively. The proposed algorithm along with a clear flow-chart is discussed in Section 5. Results illustrating the performance of the proposed approach is provided in Section 6. Finally, Section 7 provides the concluding remarks.

2 Dynamic model of the digital twin

In this section, we present the nominal dynamic system and the DT corresponding to this model. The nominal model is the ‘initial model’ of a DT. For structural engineering, we can consider a nominal model to be a numerical model of the system when it is manufactured. A DT encapsulates the journey from the nominal model to its updates based on the data collected from the system. In this section, the key ideas for developing DT of nonlinear MDOF systems are explained.

2.1 Stochastic nonlinear MDOF system: the nominal model

Consider an N –DOF stochastic nonlinear system having governing equations as follows:

$$\mathbf{M}_0 \ddot{\mathbf{X}} + \mathbf{C}_0 \dot{\mathbf{X}} + \mathbf{K}_0 \mathbf{X} + \mathbf{G}(\mathbf{X}, \alpha) = \mathbf{F} + \Sigma \dot{\mathbf{W}}, \quad (1)$$

where $\mathbf{M}_0 \in \mathbb{R}^{N \times N}$, $\mathbf{C}_0 \in \mathbb{R}^{N \times N}$ and $\mathbf{K}_0 \in \mathbb{R}^{N \times N}$, respectively, represent the mass, damping and (linear) stiffness matrix of the system. $\mathbf{G}(\cdot, \cdot) \in \mathbb{R}^N$, on the other hand, represents the nonlinearity present in the system. \mathbf{F} in Eq. (1) represents the deterministic force and $\dot{\mathbf{W}}$ (Wiener derivative) is the stochastic load vector with noise intensity matrix Σ . α in Eq. (1) represents the parameters corresponding to the nonlinear stiffness model. Note that \mathbf{M}_0 , \mathbf{C}_0 and \mathbf{K}_0 are the nominal parameters and represents the pristine system.

2.2 The digital twin

The DT for the N-DOF nonlinear system discussed above can be represented as:

$$\mathbf{M}(t_s) \frac{\partial^2 \mathbf{X}(t, t_s)}{\partial t^2} + \mathbf{C}(t_s) \frac{\partial \mathbf{X}(t, t_s)}{\partial t} + \mathbf{K}(t_s) \mathbf{X}(t, t_s) + \mathbf{G}((t, t_s), \boldsymbol{\alpha}) = \mathbf{F}(t, t_s) + \boldsymbol{\Sigma} \dot{\mathbf{W}}, \quad (2)$$

where t represents the system's time and t_s is the service time (operational time-scale). Note that the response vector \mathbf{X} is function of both the time-scales and hence, partial derivatives have been used in Eq. (2). Eq. (2) is considered to be the DT for the nominal system in Section 2.1. Eq. (2) has two time-scales, t and t_s . For all practical purposes the service time-scale t_s is much slower (in months) as compared to the time-scale of the system dynamics.

2.3 Problem statement

Although a physics-based DT for MDOF nonlinear system is defined in Eq. (2), for using it in practice, one needs to estimate the system parameters $\mathbf{M}(t_s)$, $\mathbf{C}(t_s)$ and $\mathbf{K}(t_s)$. For estimating these parameters, the connectivity between the physical twin and the DT is the key. Recent developments in IoT provides several new technologies that ensure the connectivity between the two twins. To be specific, the two-way connectivity between the DT and its counterpart is created by using sensors and actuators. Given the huge difference in the two times-scales in Eq. (2), it is reasonable to assume that the temporal variation in $\mathbf{M}(t_s)$, $\mathbf{C}(t_s)$ and $\mathbf{K}(t_s)$ are so slow that the dynamics is practically decoupled from these parametric variations. The sensor collects data intermittently at discrete time instants t_s . At each time instant t_s , time history measurements of acceleration response in $t_s \pm \Delta t$ is available. For this study, it is assumed that there is no practical variation in the mass matrix and hence, $\mathbf{M}(t_s) = \mathbf{M}_0$. Variation in damping matrix is also not considered. With this setup, the objective is to develop a DT for nonlinear MDOF system. It is envisioned that the DT should be able to track the variation in the system parameters, $\mathbf{K}(t_s)$ at current time t and is also able to predict future degradation/variation in system parameters. Last but not the least, a DT should be continuously updated as and when it receives data.

3 Bayesian Filters

One of the key components in development of DT is estimating $\mathbf{K}(t_s)$ given the observations until time t_s . This is a classical parameter estimation problem and this work proposes the use of Bayesian filter to accomplish the goal. However, one must note that development of DT and parameter estimation are not same; instead, parameter estimation is only a component of the the overall DT.

Bayesian filters use Bayesian inference to develop a framework which can then be used for state-parameter estimation. Bayesian inference differs from conventional frequentist approach of statistical inference because it takes probability of an event as the uncertainty of the event in a single trial, as opposed to the proportion of the event in a probability space. For filtering equations, let the unknown vector be given as $\mathbf{Y}_{0:T} = \{\mathbf{Y}_0, \mathbf{Y}_1, \dots, \mathbf{Y}_T\}$ which is observed through a set of noisy measurements $\mathbf{Z}_{1:T} = \{\mathbf{Z}_1, \mathbf{Z}_2, \dots, \mathbf{Z}_T\}$. Using Bayes's rule,

$$p(\mathbf{Y}_{0:T} | \mathbf{Z}_{1:T}) = \frac{p(\mathbf{Z}_{1:T} | \mathbf{Y}_{0:T}) p(\mathbf{Y}_{0:T})}{p(\mathbf{Z}_{1:T})}. \quad (3)$$

This full posterior formulation although accurate is computationally heavy and is often intractable. The computational complexity is simplified by using the first order Markovian assumption. First order Markov model assumes (i) the state of system at time step k (i.e. \mathbf{Y}_k) given the state at time step $k-1$ (i.e. \mathbf{Y}_{k-1}) is independent of anything that has happened before time step $k-1$ and (ii) The measurement at time step k (i.e. \mathbf{Z}_k) given the state at time step k (i.e. \mathbf{Y}_k) is independent of any measurement or state histories. Mathematically, this is represented as:

$$p(\mathbf{Y}_k | \mathbf{Y}_{1:k-1}, \mathbf{Z}_{1:k-1}) = p(\mathbf{Y}_k | \mathbf{Y}_{k-1}), \quad (4)$$

and

$$p(\mathbf{Z}_k | \mathbf{Y}_{1:k}, \mathbf{Z}_{1:k-1}) = p(\mathbf{Z}_k | \mathbf{Y}_k). \quad (5)$$

A probabilistic graphical model representing the first-order Markov assumption is shown in Fig. 1. In literature, this is also known as the state-space model (if the state is continuous) or the hidden Markov model (if the state is discrete). Using assumptions of Markovian model, the recursive Bayesian filter can be set up, and Kalman Filter arises [21, 35], which is a special case of recursive Bayesian filter used for linear models. Extended Kalman Filter [21], Unscented Kalman Filter (UKF) [21, 34] are improvements over Kalman filter, which are used for non-linear models. In this work, UKF is used as the Bayesian filtering algorithm of choice. It is to be noted that UKF is computationally expensive as compared to the EKF algorithm; however, the performance of UKF for systems having higher order of non-linearity is superior [34].

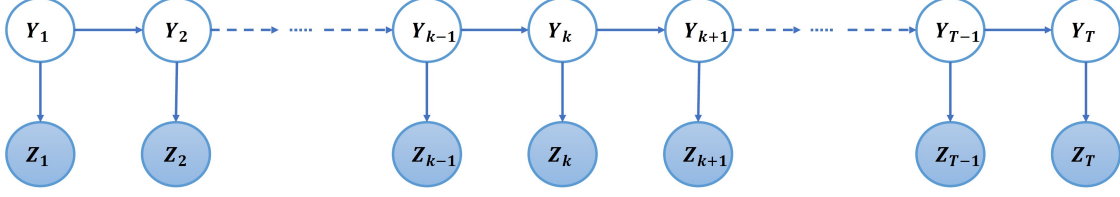


Figure 1: Probabilistic graphical model for state space model. We have considered first order Markovian assumption for the hidden variable \mathbf{Y} ; this ensures that \mathbf{Y}_t is only dependent on \mathbf{Y}_{t-1} .

3.1 Unscented Kalman Filter

UKF uses concepts of unscented transform to analyze non-linear models and directly tries to approximate the mean and co-variance of the targeted distribution instead of approximating the non-linear function. To that end, weighted sigma points are used. The idea here is to consider some points on the source Gaussian distribution which are then mapped onto the target Gaussian distribution after passing through non-linear function. These points are referred to as the sigma points and are considered to be representative of the transformed Gaussian distribution. Considering L to be the length of the state vector, $2L + 1$ sigma points are selected as [34],

$$\begin{aligned} \mathcal{Y}^{(0)} &= \boldsymbol{\mu} \\ \mathcal{Y}^{(i)} &= \boldsymbol{\mu} + \sqrt{(L + \lambda)} \begin{bmatrix} \sqrt{\boldsymbol{\Sigma}} \end{bmatrix}, \quad i = 1, \dots, L \\ \mathcal{Y}^{(i)} &= \boldsymbol{\mu} - \sqrt{(L + \lambda)} \begin{bmatrix} \sqrt{\boldsymbol{\Sigma}} \end{bmatrix}, \quad i = L + 1, \dots, 2L, \end{aligned} \quad (6)$$

where, \mathcal{Y} are the required sigma points, $\boldsymbol{\mu}$ and $\boldsymbol{\Sigma}$ are, respectively the mean vector and co-variance matrix. λ and L in Eq. (6) represent the scaling parameter and length of state vector respectively. Details on how to compute λ is explained while discussing the UKF algorithm. Once the mean m_k and covariance p_k , are computed using the UKF, we approximate the filtering distribution as:

$$p(y_k | z_{1:k}) \simeq N(y_k | m_k, p_k), \quad (7)$$

where m_k and p_k are the mean and co-variance computed by the algorithm discussed next. A schematic representation of how sigma points are used within the UKF algorithm is shown in Fig. 2

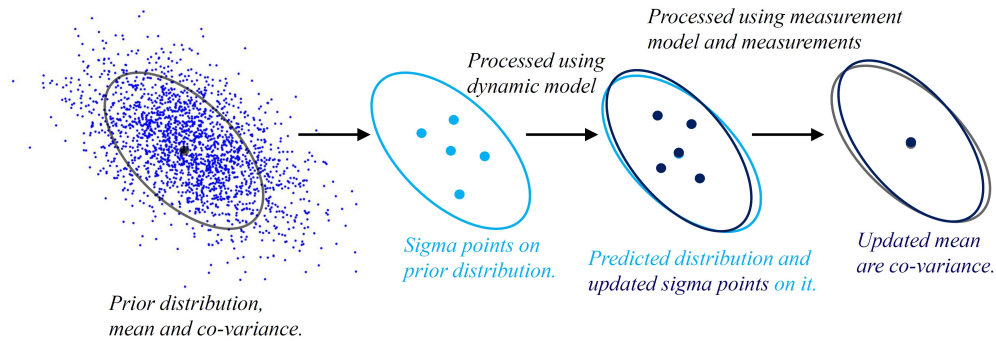


Figure 2: Schematic representation of functionality of sigma points within the UKF framework.

3.1.1 Algorithm

Step 1 Weights calculation for sigma points

Select UKF parameters : $\alpha_f = 0.001, \beta = 2, \kappa = 0$

$$\begin{aligned} W_m^{(i=0)} &= \frac{\lambda}{L + \lambda} \\ W_c^{(i=0)} &= \frac{\lambda}{L + \lambda} + (1 - \alpha_f^2 + \beta), \quad i = 1, \dots, 2L \\ W_m^{(i)} &= \frac{1}{2(L + \lambda)} \\ W_c^{(i)} &= W_m^{(i)}, \quad i = 1, \dots, 2L, \end{aligned} \quad (8)$$

where, L is the length of state vector and scaling parameter $\lambda = \alpha_f^2(L + \kappa) - L$.

Step 2 : For $k = 0$

Initialize mean and co-variance i.e. $m_k = m_0, p_k = p_0$.

Step 3 : For $k = 1, 2, \dots, t_n$

Step 3.1 : Prediction

Getting Sigma points $\mathcal{Y}^{(i)}, i = 0, \dots, 2L$

$$\begin{aligned} \mathcal{Y}_{k-1}^{(0)} &= m_{k-1} \\ \mathcal{Y}_{k-1}^{(i)} &= m_{k-1} + \sqrt{L + \lambda} \begin{bmatrix} \sqrt{P_{k-1}} \end{bmatrix} \\ \mathcal{Y}_{k-1}^{(i+L)} &= m_{k-1} - \sqrt{L + \lambda} \begin{bmatrix} \sqrt{P_{k-1}} \end{bmatrix}, \quad i = 1, \dots, L. \end{aligned} \quad (9)$$

Propagate sigma points through the dynamic model

$$\mathcal{Y}_k^{(i)} = f(\mathcal{Y}_{k-1}^{(i)}), \quad i = 0, \dots, 2L. \quad (10)$$

The predicted mean m_k^- and co-variance P_k^- is then given by

$$\begin{aligned} m_k^- &= \sum_{i=0}^{2L} W_m^{(i)} \mathcal{Y}_k^{(i)}, \\ P_k^- &= \sum_{i=0}^{2L} W_c^{(i)} (\mathcal{Y}_k^{(i)} - m_k^-)(\mathcal{Y}_k^{(i)} - m_k^-)^T + Q_{k-1}. \end{aligned} \quad (11)$$

Step 3.2 : Update

Getting Sigma points

$$\begin{aligned} \mathcal{Y}_k^{-(0)} &= m_k^- \\ \mathcal{Y}_k^{-(i)} &= m_k^- + \sqrt{L + \lambda} \begin{bmatrix} \sqrt{P_k^-} \end{bmatrix} \\ \mathcal{Y}_k^{-(i+L)} &= m_k^- - \sqrt{L + \lambda} \begin{bmatrix} \sqrt{P_k^-} \end{bmatrix}, \quad i = 1, \dots, L. \end{aligned} \quad (12)$$

Propagating sigma points through the measurement model

$$\mathcal{Z}_k^{(i)} = h(\mathcal{Y}_k^{-(i)}), \quad i = 0, \dots, 2L. \quad (13)$$

Getting mean μ_k , predicted co-variance S_k and cross co-variance C_k

$$\begin{aligned} \mu_k^- &= \sum_{i=0}^{2L} W_m^{(i)} \mathcal{Z}_k^{(i)}, \\ S_k^- &= \sum_{i=0}^{2L} W_c^{(i)} (\mathcal{Z}_k^{(i)} - \mu_k^-)(\mathcal{Z}_k^{(i)} - \mu_k^-)^T + R_k, \\ C_k^- &= \sum_{i=0}^{2L} W_c^{(i)} (\mathcal{Y}_k^{-(i)} - m_k^-)(\mathcal{Z}_k^{(i)} - \mu_k^-)^T. \end{aligned} \quad (14)$$

Step 3.3 : Getting filter gain K_k , filtered state mean m_k and co-variance P_k conditional on measurement y_k .

$$\begin{aligned} K_k &= C_k S_k^{-1}, \\ m_k &= m_k^- + K_k [y_k - \mu_k], \\ P_k &= P_k^- - K_k S_k K_k^T. \end{aligned} \quad (15)$$

Within the DT framework, the UKF algorithm is used for parameter estimation at a given time-step, t_k .

4 Gaussian Process Regression

In this section, we briefly discuss the other component of the proposed DT framework, namely Gaussian process regression (GPR). GPR [15, 28], along with neural network [36, 37] are perhaps the most popular machine learning techniques in today's time. Unlike conventional frequentist machine learning techniques, GPR doesn't assume a functional form to represent input-output mapping; instead, a distribution over a function is assumed in GPR. Consequently, GPR has the inherent capability of capturing the epistemic uncertainty [38] arising due to limited data. This feature of GPR is particularly useful when it comes to decision making. Within the proposed DT framework, we use GPR to track the temporal evolution of the system parameters.

We consider v_k to be the systems parameters and time τ_k . In GPR, we represent v_k as

$$v_k \sim \mathcal{GP}(\mu(\tau_k; \beta), \kappa(\tau_k, \tau'_k; \sigma^2, \mathbf{l})), \quad (16)$$

where $\mu(\cdot; \beta)$ and $\kappa(\cdot, \cdot; \sigma^2, \mathbf{l})$, respectively represent the mean function and the covariance function of the GPR. The mean function is parameterized by the unknown coefficient vector β and the covariance function is parameterized by the process variance σ^2 and the length-scale parameters \mathbf{l} . All the parameters combined, $\theta = [\beta, \mathbf{l}, \sigma^2]$ are known as hyperparameters of GPR. It is worthwhile to note that choice of $\mu(\cdot; \beta)$ and $\kappa(\cdot, \cdot; \sigma^2, \mathbf{l})$ has significant influence on the performance of GP; this naturally allows an user to encode prior knowledge into the GPR model and model complex functions [15]. In case there is no prior knowledge about the mean function, it is a common practice to use zero mean Gaussian process,

$$v_k \sim \mathcal{GP}(\mathbf{0}, \kappa(\tau_k, \tau'_k; \sigma^2, \mathbf{l})). \quad (17)$$

The covariance function $\kappa(\cdot, \cdot; \sigma^2, \mathbf{l})$, on the other hand, should result in a positive, semi-definite matrix. For using the GPR in practice, one needs to compute the hyperparameters θ based on training samples $\mathcal{D} = [\tau_k, v_k]_{k=1}^{N_s}$ where N_s is the number of training samples. The most widely used method in this regards is based on the maximum likelihood estimation where the negative log-likelihood of GPR is minimized. For details on MLE for GPR, interested readers may refer [39]. The other alternative is to compute the posterior distribution of hyperparameter vector θ [28, 29]. This although a superior alternative, renders the process computationally expensive. In this work, we have used the MLE based approach because of this simplicity. For ease of readers, the steps involved in training a GPR model are shown in Algorithm 1.

Once the hyper-parameters θ are computed, predictive mean and predictive variance corresponding to new input τ^* are computed as

$$\mu^* = \Phi \beta^* + \kappa^*(\tau^*; (\sigma^*)^2, \mathbf{l}^*) \mathbf{K}^{-1} (\mathbf{v} - \Phi \beta^*), \quad (18)$$

$$s^2(\tau^*) = (\sigma^*)^2 \left\{ 1 - \kappa^*(\tau^*; (\sigma^*)^2, \theta^*) \mathbf{K}^{-1} \kappa^*(\tau^*; (\sigma^*)^2, \mathbf{l}^*)^T + \frac{[1 - \Phi^T \mathbf{K}^{-1} \kappa^*(\tau^*; (\sigma^*)^2, \mathbf{l}^*)^T]}{\Phi^T \mathbf{K}^{-1} \Phi} \right\}, \quad (19)$$

where β^* , \mathbf{l}^* and σ^* represents the optimized hyper-parameters. Φ in Eqs. (18) and (19) represents the design matrix. $\kappa^*(\tau^*; (\sigma^*)^2, \mathbf{l}^*)^T$ in Eqs. (18) and (19) are the covariance vector between the input training samples and τ^* and computed as

$$\kappa^*(\tau^*; (\sigma^*)^2, \mathbf{l}^*)^T = [\kappa(\tau^*, \tau_1; (\sigma^*)^2, \theta^*), \dots, \kappa(\tau^*, \tau_{N_s}; (\sigma^*)^2, \theta^*)]. \quad (20)$$

5 Proposed approach

Having discussed UKF and GP, the two ingredients of the proposed approach, we proceed to discussing the proposed DT framework for nonlinear dynamical systems. A schematic representation of the proposed DT is shown in Fig. 3. It has four primary components, namely (a) selection of nominal model, (b) data collection, (c) parameter estimation

Algorithm 1: Training GPR

- 1 **Pre-requisite:** Form of mean function $\mu(\cdot; \beta)$ and covariance function, $\kappa(\cdot, \cdot; \sigma^2, 1)$. Provide training data, $\mathcal{D} = [\tau_k, \mathbf{v}_k]_{k=1}^{N_s}$, initial values of the parameters, θ_0 , maximum allowable iteration n_{max} and error threshold ϵ_t .
- 2 $\theta \leftarrow \theta_0$; $iter \leftarrow 0$; $\epsilon \leftarrow 10\epsilon_t$
- 3 **repeat**
- 4 $iter \leftarrow iter + 1$
- 5 $\theta_{iter-1} \leftarrow \theta$.
- 6 Compute the negative log-likelihood by using the training data \mathcal{D} and θ

$$f_{ML} \propto \frac{1}{N} \left| \mathbf{K}(\theta) + \log \left(\mathbf{v}^T \mathbf{R}(\theta)^{-1} \mathbf{v} \right) \right|,$$

where $\mathbf{K}(\theta)$ is the covariance matrix computed by using the training data and covariance function $\kappa(\cdot, \cdot; \sigma^2, 1)$. \mathbf{v} represents the observation vector.
- 7 Update hyperparameter θ based on the gradient information.
- 8 $\theta_{iter} \leftarrow \theta$.
- 9 $\epsilon \leftarrow \|\theta_{iter} - \theta_{iter-1}\|_2^2$
- 10 **until** $iter \geq n_{max}$ and $\epsilon > \epsilon_t$;
- 11 **Output:** Optimal hyper-parameter, θ^*

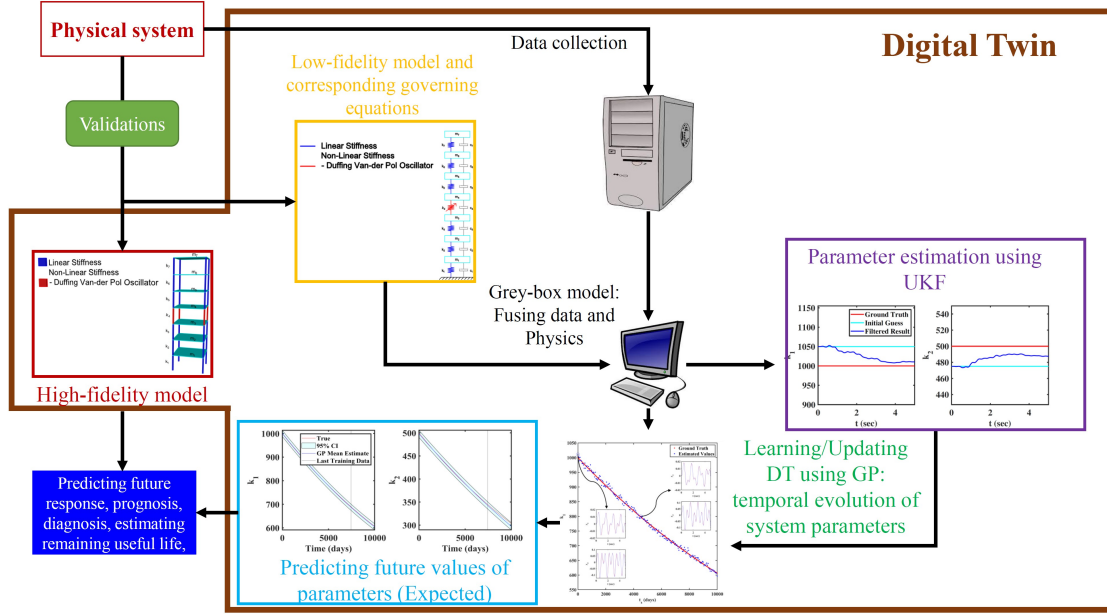


Figure 3: Schematic representation of the proposed digital twin framework. It comprises of low-fidelity model as nominal model, UKF for parameter estimation, GP for learning temporal evolution of parameters and predicting future values of system parameters, and high-fidelity model for estimating future responses.

at a given time-instant and (d) estimation of the temporal variation in parameters. The selection of nominal model has already been detailed in Section 2 and hence, here the discussion is limited to data collection, parameter estimation and estimation of temporal variation of the parameters only.

One major concern in DT is its connectivity with the physical counterpart; in absence of which, a DT will be of no practical use. To ensure connectivity, sensors are placed on the physical system (physical twin) for data collection. The data is communicated to the DT by using cloud technology. With the substantial advancements in IoT, the access to different types of sensors is straightforward for collecting different types of data. In this work, we have considered that accelerometers are mounted on the physical system and the DT receives acceleration measurements. To be specific, one can consider that the acceleration time-history are available to the DT intermittently at discrete time-instant t_s . Note that the proposed approach is equally applicable (with trivial modifications) if instead of acceleration, displacement

or velocity measurements are available. The framework can also be extended to function in tandem with vision based sensors. However, from a practical and economic point-of-view, it is easiest to collect acceleration measurements and hence, the same has been considered in this study.

Once the data is collected, the next objective is to estimate the system parameters (stiffness matrix to be specific), assuming that at time-instant t_s , acceleration measurements are available in $[t_s - \Delta t, t_s]$, where Δt is time interval over which acceleration measurement is available at t_s . It is to be noted that t_s is a time-step in the slow time-scale whereas Δt is time interval in the fast time-scale. With this setup, the parameter estimation objective is to estimate $\mathbf{K}(t_s)$. In this work, we estimate $\mathbf{K}(t_s)$ by using the UKF. Details on how parameter estimation is carried out using UKF is elaborated in Section 3.

The last step within the proposed DT framework is to estimate the temporal evolution of the parameters. This is extremely important as it enables the DT to predict future behavior of the physical system. In this work, we propose to use a combination of GPR and UKF for learning the temporal evolution of the system parameters. To be specific, consider $\mathbf{t} = [t_1, t_2, \dots, t_N]$ to be time-instants in slow-scale. Also, assume that using UKF, the estimated the system parameters are available at different time-instants as $\mathbf{v} = [\mathbf{v}_1, \mathbf{v}_2, \dots, \mathbf{v}_N]$, where \mathbf{v}_i includes the elements of stiffness matrix. The proposed work trains a GPR model between \mathbf{t} and \mathbf{v} ,

$$\mathbf{v} \sim \mathcal{GP}(\boldsymbol{\mu}, \boldsymbol{\kappa}). \quad (21)$$

Note that for brevity, the hyperparameters in Eq. (21) are omitted. The GPR is trained by following the procedure discussed in Algorithm 1. Once trained, the GPR can predict the system parameters at future time-steps. Note that GPR being a Bayesian machine learning model also provides the predictive uncertainty which can be used to judge the accuracy of the model. For the ease of readers, the overall DT framework proposed is shown in Algorithm 2.

Algorithm 2: Proposed DT

- 1 Select nominal model ; ▷ Section 2
 - 2 . Use data (acceleration measurements) \mathcal{D}_s collected at time t_s to compute the parameters $\mathbf{K}(t_s)$; ▷ Section 3
 - 3 . Train a GP using $\mathcal{D} = [t_n, \mathbf{v}_n]_{n=1}^{t_s}$ as training data, where \mathbf{v}_n represents the system parameter ; ▷ Algorithm 1
 - 4 . Predict $\mathbf{K}(\tilde{t})$ at future time \tilde{t} ; ▷ Section 4
 - 5 Substitute $\mathbf{K}(\tilde{t})$ into the governing equation (high-fidelity model) and solve it to obtain responses at time \tilde{t} .
 - 6 Take decisions related to maintenance, remaining useful life and health of the system.
 - 7 Repeat steps 2 – 6 as more data become available
-

6 Numerical Illustrations

In this section, we present two examples to illustrate the performance of the proposed DT framework. The first example selected is a 2-DOF system with duffing oscillator attached at the first floor. As the second example, a 7-DOF system is considered. For this example, the nonlinearity in the system arises because of a duffing van der pol oscillator attached between the third and the fourth DOF. As stated earlier, we have considered that acceleration measurements at different time-steps are available. The objective here is to use the proposed DT to compute the time-evolution of the system parameters. Once the time-evolution of the parameters are known, the proposed DT can be used for predicting the responses of the system at future time-steps (t_s) (see Algorithm 2 for details). In this section, we have illustrated how the proposed approach can be used for predicting the time-evolution of the system parameters in the past as well as in the future.

6.1 2-DOF system with duffing oscillator

As the first example, we consider a 2-DOF system as shown in Fig. 4. The nonlinear duffing oscillator is attached with the first degree of freedom. The coupled governing equations for this system are represented as

$$\begin{aligned} m_1 \ddot{x}_1 + c_1 \dot{x}_1 + k_1 x_1 + \alpha_{DO} x_1^3 + c_2 (\dot{x}_1 - \dot{x}_2) + k_2 (x_1 - x_2) &= \sigma_1 \dot{W}_1 + f_1, \\ m_2 \ddot{x}_2 + c_2 (\dot{x}_2 - \dot{x}_1) + k_2 (x_2 - x_1) &= \sigma_2 \dot{W}_2 + f_2, \end{aligned} \quad (22)$$

where m_i , c_i and k_i , respectively, represent the mass, damping and stiffness of the i -th degree of freedom. Although not explicitly shown, it is to be noted that k_i changes with the slow time-scale t_s . F_i and $\sigma_i \dot{W}_i$, respectively, represents the deterministic and the stochastic force acting on the i -th floor. α_{DO} controls the nonlinearity in the system. The parametric values considered for this example are shown in Table 1.

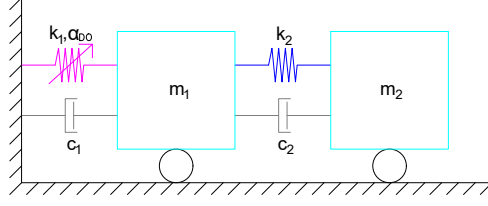


Figure 4: Schematic representation of the 2-DOF System with duffing oscillator considered in example 1. The nonlinear duffing oscillator is attached with the first degree of freedom (shown in magenta).

Table 1: System Parameters for 2-DOF System

Mass (Kg)	Stiffness Constant (N/m)	Damping Constant (Ns/m)	Force(N) $F_i = \lambda_i \sin(\omega_i t)$	Stochastic Noise Parameters
$m_1 = 20$	$k_1 = 1000$	$c_1 = 10$	$\lambda_1 = 10, \omega_1 = 10$	$s_1 = 0.1$
$m_2 = 10$	$k_2 = 500$	$c_2 = 5$	$\lambda_2 = 10, \omega_2 = 10$	$s_2 = 0.1$
DO Oscillator Constant, $\alpha_{DO} = 100$				

The system states are defined as:

$$\begin{aligned} x_1 &= y_1, & x_2 &= y_2, \\ \dot{x}_1 &= y_3, & \dot{x}_2 &= y_4, \end{aligned} \quad (23)$$

and the governing equation in Eq. (22) is represented in the form of Ito-diffusion equations to obtain the drift and dispersion coefficients:

$$d\mathbf{y} = \mathbf{a} dt + \mathbf{b} d\mathbf{W}, \quad (24)$$

where

$$\mathbf{a} = \begin{bmatrix} y_3 \\ y_4 \\ \frac{f_1}{m_1} - \frac{1}{m_1} (c_1 y_3 + c_2 y_3 - c_2 y_4 + k_1 y_1 + k_2 y_1 - k_2 y_2 + \alpha_{do} y_1^3) \\ \frac{1}{m_2} (c_2 y_3 - c_2 y_4 + k_2 y_1 - k_2 y_2 m_2) + \frac{f_2}{m_2} \end{bmatrix} \quad (25a)$$

$$\mathbf{b} = \begin{bmatrix} 0 & 0 \\ 0 & 0 \\ \frac{\sigma_1}{m_1} & 0 \\ 0 & \frac{\sigma_2}{m_2} \end{bmatrix}. \quad (25b)$$

For illustrating the performance of the proposed digital twin, we generate synthetic data by simulating Eq. (24). The data simulation is carried out using Taylor 1.5 strong scheme [17, 40]

$$\begin{aligned} \mathbf{y}_{k+1} &= (\mathbf{y} + \mathbf{a}\Delta t + \mathbf{b}\Delta\mathbf{w} + 0.5L^j(\mathbf{b})(\Delta w^2 - \Delta t) + L^j(\mathbf{a})\Delta\mathbf{z} \\ &\quad + L^0(\mathbf{b})(\Delta w\Delta t - \Delta z) + 0.5L^0(\mathbf{a})\Delta t^2)_k \end{aligned} \quad (26)$$

where, L^0 and L^j are Kolmogorov operators [40] evaluated on drift and diffusion coefficients i.e. on elements of \mathbf{a} and \mathbf{b} . $\Delta\mathbf{w}$ and $\Delta\mathbf{z}$ are the Brownian increments [40] evaluated at each time step Δt . Before proceeding with the performance of the proposed DT, we investigate the performance of UKF in joint parameter state estimation. To avoid the so called ‘inverse crime’ [41], Euler Maruyama (EM) integration scheme is used during filtering.

$$\mathbf{y}_{k+1} = (\mathbf{y} + \mathbf{a}\Delta t + \mathbf{b}\Delta\mathbf{w})_k. \quad (27)$$

It may be noted that EM integration scheme provides a lower-order approximation as compared to Taylor’s 1.5 strong integration scheme. In other words, the data is generated using a more accurate scheme as compared to the filtering. This helps in emulating a realistic scenario. For combined state-parameter estimation, the state space vector is modified as $\mathbf{y} = [y_1 \ y_2 \ y_3 \ y_4 \ k_1 \ k_2]^T$. Consequently, \mathbf{a} and \mathbf{b} are also modified as:

$$\mathbf{a} = \begin{bmatrix} y_3 \\ y_4 \\ \frac{f_1}{m_1} - \frac{1}{m_1} (c_1 y_3 + c_2 y_3 - c_2 y_4 + k_1 y_1 + k_2 y_1 - k_2 y_2 + \alpha_{do} y_1^3) \\ \frac{1}{m_2} (c_2 y_3 - c_2 y_4 + k_2 y_1 - k_2 y_2) + \frac{f_2}{m_2} \\ 0 \\ 0 \end{bmatrix}, \quad (28a)$$

$$\mathbf{b} = \begin{bmatrix} 0 & 0 \\ 0 & 0 \\ \frac{\sigma_1}{m_1} & 0 \\ 0 & \frac{\sigma_2}{m_2} \\ 0 & 0 \\ 0 & 0 \end{bmatrix}. \quad (28b)$$

For obtaining the dynamic model function for UKF model, first two terms of EM algorithm are used.

$$\mathbf{f}(\mathbf{y}) = \mathbf{y} + \mathbf{a}\Delta t. \quad (29)$$

For estimating the noise covariance \mathbf{Q} , q is expressed as:

$$\mathbf{q} = \mathbf{q}_c \mathbf{R} \mathbf{V}, \quad (30)$$

where \mathbf{q}_c is a constant diagonal matrix which is multiplied by vector of random variables $\mathbf{R} \mathbf{V}$ to compute \mathbf{q} . The basic form for \mathbf{q}_c is extracted from the remaining terms of EM algorithm i.e., $\mathbf{b}\Delta w$.

$$\mathbf{q}_c = \text{diag} \left[0 \quad 0 \quad \frac{\sigma_1 \sqrt{\Delta t}}{m_1} \quad \frac{\sigma_2 \sqrt{\Delta t}}{m_2} \quad 0 \quad 0 \right], \quad (31)$$

$$\mathbf{Q} = \mathbf{q}_c \mathbf{q}_c^T.$$

The individual terms of \mathbf{Q} can then be modified by any suitable factor to improve the accuracy of the filter. Considering that the acceleration measurements are available to the DT, the simulated acceleration measurements are obtained as follows:

$$\mathbf{A} = -\mathbf{M}^{-1}(\mathbf{G} + \mathbf{K}\mathbf{X} + \mathbf{C}\dot{\mathbf{X}}), \quad (32)$$

where \mathbf{M} , \mathbf{C} and \mathbf{K} are the mass, damping and stiffness matrices. \mathbf{G} , as already discussed in Eq. (1) is the contribution due to the nonlinearity in the system. Eq. (32) can be written in the state-space form as

$$\mathbf{A} = \begin{bmatrix} -\frac{1}{m_1} (c_1 y_3 + c_2 y_3 - c_2 y_4 + k_1 y_1 + k_2 y_1 - k_2 y_2 + \alpha_{do} y_1^3) \\ \frac{1}{m_2} (c_2 y_3 - c_2 y_4 + k_2 y_1 - k_2 y_2) \end{bmatrix}. \quad (33)$$

Using Eq. 33, the observation/measurement model for the UKF can be written as

$$\mathbf{h}(\mathbf{y}) = \begin{bmatrix} -\frac{1}{m_1} (c_1 y_3 + c_2 y_3 - c_2 y_4 + k_1 y_1 + k_2 y_1 - k_2 y_2 + \alpha_{do} y_1^3) \\ \frac{1}{m_2} (c_2 y_3 - c_2 y_4 + k_2 y_1 - k_2 y_2) \end{bmatrix}. \quad (34)$$

The simulated acceleration measurements are corrupted by white Gaussian noise having a signal-to-noise ratio (SNR) of 50, where SNR is defined as: $\text{SNR} = \sigma_{\text{signal}}^2 / \sigma_{\text{noise}}^2$ and σ is the standard deviation. The deterministic force vector is also corrupted by white Gaussian noise having SNR of 20. Representative examples of acceleration and deterministic force for this problem are shown in Fig. 5. We use UKF along with the acceleration and deterministic force measurements, $\mathbf{f}(\mathbf{y})$ and $\mathbf{h}(\mathbf{y})$ for combined parameter state estimation. Fig. 7 shows the combined state

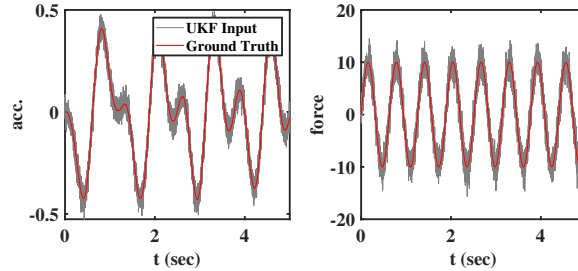


Figure 5: Sample Acceleration and deterministic component of the force for the 2-DOF problem. The stochasticity observed for the force is due to the noise present. Note that there is an additional stochastic component of force as shown in Eq. (27).

parameter estimation results for first data point i.e. $t_{s(i)} = t_{s(1)}$ of 2-DOF system. This is a relatively simple case where measurements at both degrees of freedom are available (see Fig. 6). It can be observed that UKF provides highly accurate estimates of the state vectors. As for parameter estimation (see Fig. 7(b)), we observe that UKF provides highly accurate estimate for k_1 . As for k_2 , compared to the ground truth ($k_2 = 500\text{N/m}$), the proposed approach ($k_2 = 487.5\text{N/m}$) provides an accuracy of around 98%. Fig. 9 shows the result for an intermediate data point i.e. at

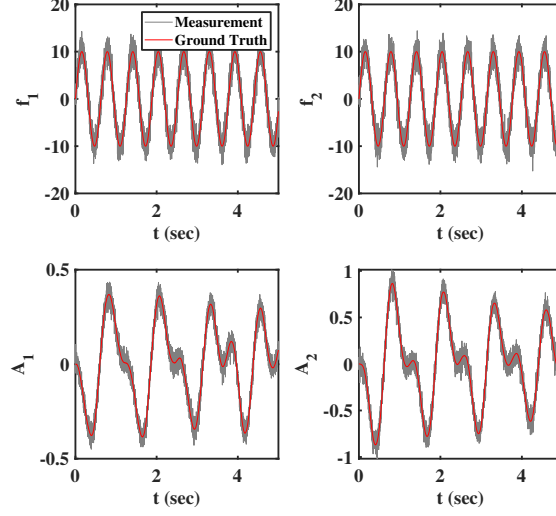
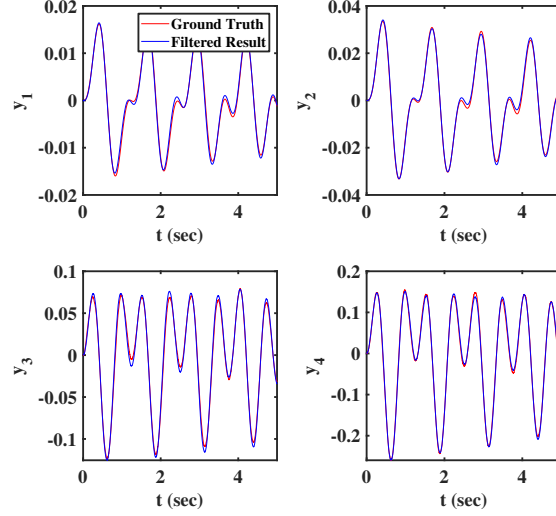
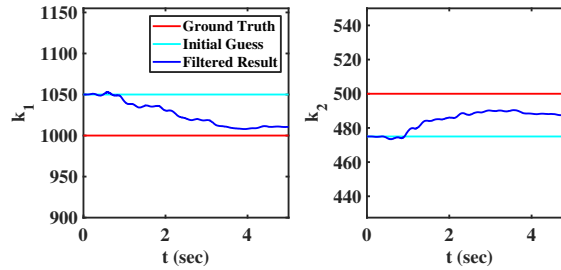


Figure 6: Deterministic component of force and acceleration vectors at the two DOFs. The noisy acceleration vectors are provided as measurement to the UKF model.



(a) State (Displacement And Velocity) Estimation



(b) Parameter (Stiffness) Estimation

Figure 7: Combined state and parameter estimation results for the 2DOF system. Noisy measurements of acceleration at both the DOFs are provided as input to the UKF algorithm. The results corresponds to the initial measurement data.

time $t_{s(i)} = t_{s(91)}$. The initial values of parameter while filtering are taken as the final values of parameter obtained from previous data point. Similar to that observed for the initial data point, Fig. 9 shows that the filter manages to estimate the states accurately and also improves upon the parameter estimation. Next, we consider a more challenging

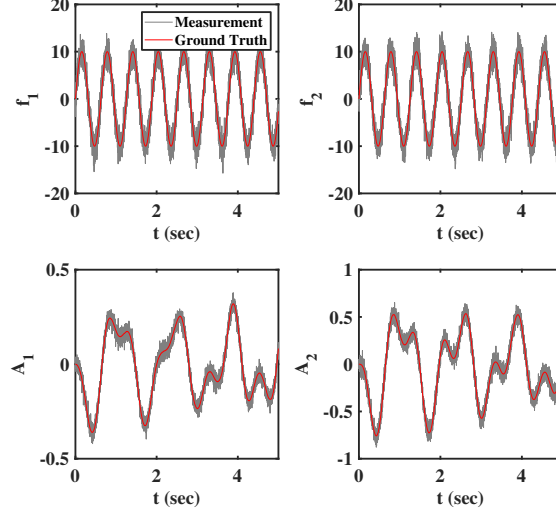
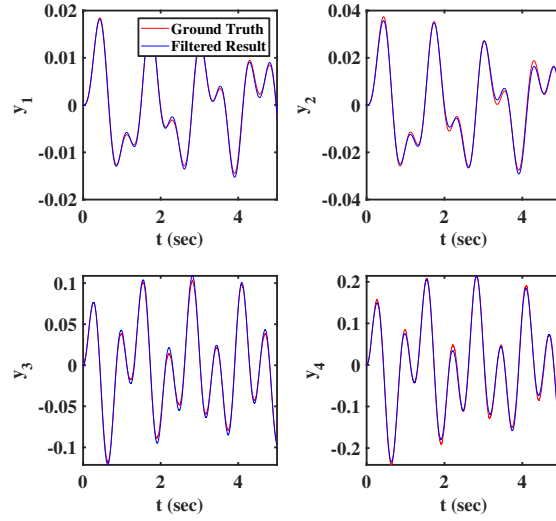
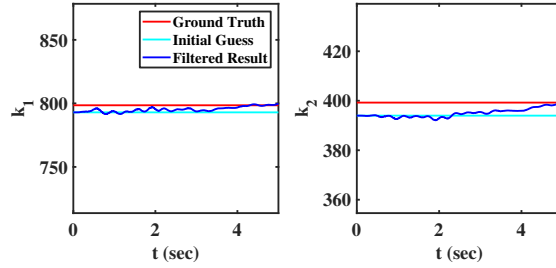


Figure 8: Force (deterministic part) and acceleration vectors at an intermediate time-step. The noisy accelerations at the 2DOFs are provided as measurements to the UKF algorithm.



(a) State (Displacement And Velocity) Estimation



(b) Parameter (Stiffness) Estimation

Figure 9: Combined state and parameter estimation results for the 2DOF system. Noisy measurements of acceleration at both the DOFs are provided as input to the UKF algorithm. The results corresponds to an intermediate measurement data.

scenario where data at only one DOF is available. To be specific, acceleration measurements at DOF-1 is considered

to be available (see Fig. 10). This changes the measurement model $h(\cdot)$ while filtering and reduce it to,

$$h(y) = -\frac{1}{m_1} (c_1 y_3 + c_2 y_3 - c_2 y_4 + k_1 y_1 + k_2 y_1 - k_2 y_2 + \alpha_{do} y_1^3). \quad (35)$$

Fig. 11 shows the state and parameter estimation results for this case. Similar to previous case, it can be observed that the state estimate and the estimate for k_1 are obtained with high degree of accuracy (see Fig. 11). Estimate for k_2 also approaches the ground truth ($k_2 = 500N/m$) giving an accuracy of approximately 98%. Finally, we focus on the

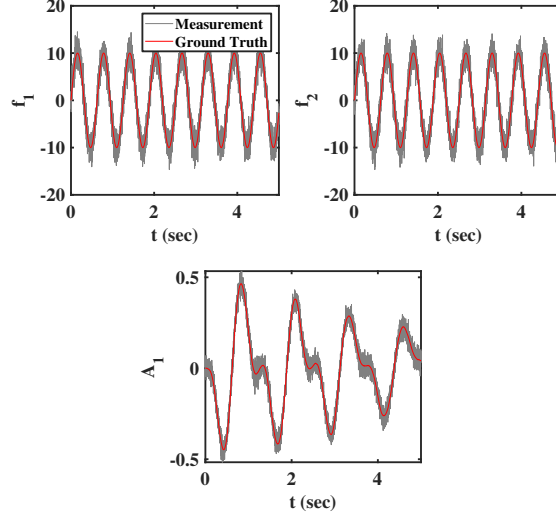


Figure 10: Deterministic component of force and acceleration vector used in UKF. For this case, only acceleration measurements at first degree of freedom is available.

other objective of the DT, which is to compute the time-evolution of the parameters, considering the stiffness to vary with slow time-scale t_s as follows.

$$k(t_s) = k_0 \delta, \quad (36)$$

where

$$\delta = e^{-0.5 \times 10^{-4} \times t_s}. \quad (37)$$

We consider that acceleration measurements are available for 5 seconds every 50 days. UKF is utilized as discussed before for computing the stiffness at each time-steps. The resulting data obtained is shown in Fig. 12. Once the data points are obtained, GP is employed to evaluate the temporal evolution of the parameters. Fig. 13 shows results obtained using GP. The vertical lines in Fig. 13 indicate the time until which data is provided to the GP. It is observed that GP yields highly accurate estimate of the two stiffness. Interestingly, results obtained using GP are not only accurate in the time-window (indicated by the vertical line) but also outside. This indicates the the proposed DT can be used for predicting the system parameters at future time-step which in-turn can be used for predicting the future responses and solving remaining useful life and predictive maintenance optimization problems. Additionally, GP being a Bayesian machine learning algorithm provides an estimate of the confidence interval. This can be used for collecting more data and in decision making.

6.2 7-DOF system with duffing van der pol oscillator

As our second example we consider a 7-DOF system as shown in Fig. 14. The 7-DOF system is modeled with a DVP oscillator at fourth DOF. The governing equations of motion for the 7-DOF system are given as,

$$\mathbf{M}\ddot{\mathbf{X}} + \mathbf{C}\dot{\mathbf{X}} + \mathbf{K}\mathbf{X} + \mathbf{G}(\mathbf{X}, \alpha) = \mathbf{F} + \mathbf{\Sigma}\dot{\mathbf{W}}, \quad (38)$$

where $\mathbf{M} = \text{diag}[m_1, \dots, m_7] \in \mathbb{R}^{7 \times 7}$, $\mathbf{X} = [x_1, \dots, x_7]^T \in \mathbb{R}^7$, $\mathbf{\Sigma} = \text{diag}[\sigma_1, \dots, \sigma_7] \in \mathbb{R}^{7 \times 7}$, $\dot{\mathbf{W}} = [\dot{W}_1, \dots, \dot{W}_7]^T \in \mathbb{R}^7$, $\mathbf{F} = [f_1, \dots, f_7]^T \in \mathbb{R}^7$ and

$$\mathbf{G} = \alpha_{DVP} [\mathbf{0}_{1 \times 3} \quad (x_3 - x_4)^3 \quad (x_4 - x_3)^3 \quad \mathbf{0}_{1 \times 2}]^T \in \mathbb{R}^7.$$

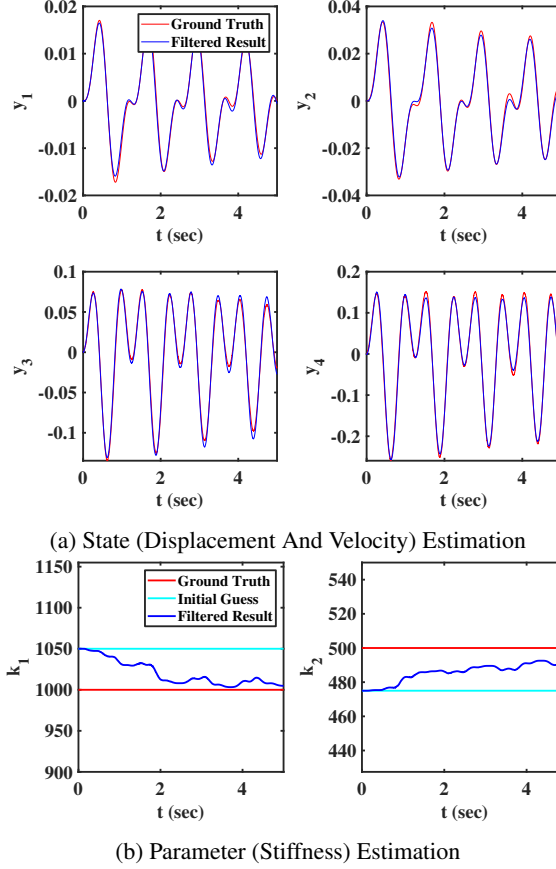


Figure 11: Combined state and parameter estimation results for the 2DOF system estimated from only one acceleration measurements. The noisy acceleration measurement at DOF 1 is provided to the UKF as measurement.

\mathbf{C} and \mathbf{K} in Eq. (38) are tri-diagonal matrices representing damping and stiffness (linear component),

$$\mathbf{C} = \begin{bmatrix} c_1 + c_2 & -c_2 & & & & & & \\ -c_2 & c_2 + c_3 & -c_3 & & & & & \\ & -c_3 & c_3 + c_4 & -c_4 & & & & \\ & & -c_4 & c_4 + c_5 & -c_5 & & & \\ & & & -c_5 & c_5 + c_6 & -c_6 & & \\ & & & & -c_6 & c_6 + c_7 & -c_7 & \\ & & & & & -c_6 & c_7 & \end{bmatrix}, \quad (39)$$

$$\mathbf{K} = \begin{bmatrix} k_1 + k_2 & -k_2 & & & & & & \\ -k_2 & k_2 + k_3 & -k_3 & & & & & \\ & -k_3 & k_3 + k_4 & -k_4 & & & & \\ & & k_4 & -k_4 + k_5 & -k_5 & & & \\ & & & -k_5 & k_5 + k_6 & -k_6 & & \\ & & & & -k_6 & k_6 + k_7 & -k_7 & \\ & & & & & -k_6 & k_7 & \end{bmatrix}, \quad (40)$$

where m_i , c_i and k_i , respectively, represent the mass, damping and stiffness of the i -th degree of freedom. We have considered the stiffness of all, but the fourth DOF to vary with the slow time-scale t_s . The rationale behind not varying the stiffness corresponding to the 4th DOF resides in the fact that nonlinear stiffness is generally used for vibration control [42] and energy harvesting [43] and hence, is kept constant. Parametric values for the 7-DOF system are shown in Table 2.

To convert the governing equations for 7 DOF system to state space equations, the following transformations are considered:

$$\begin{aligned} x_1 &= y_1, & \dot{x}_1 &= y_2, & x_2 &= y_3, & \dot{x}_2 &= y_4, & x_3 &= y_5, & \dot{x}_3 &= y_6, & x_4 &= y_7 \\ \dot{x}_4 &= y_8, & x_5 &= y_9, & \dot{x}_5 &= y_{10}, & x_6 &= y_{11}, & \dot{x}_6 &= y_{12}, & x_7 &= y_{13}, & \dot{x}_7 &= y_{14} \end{aligned} \quad (41)$$

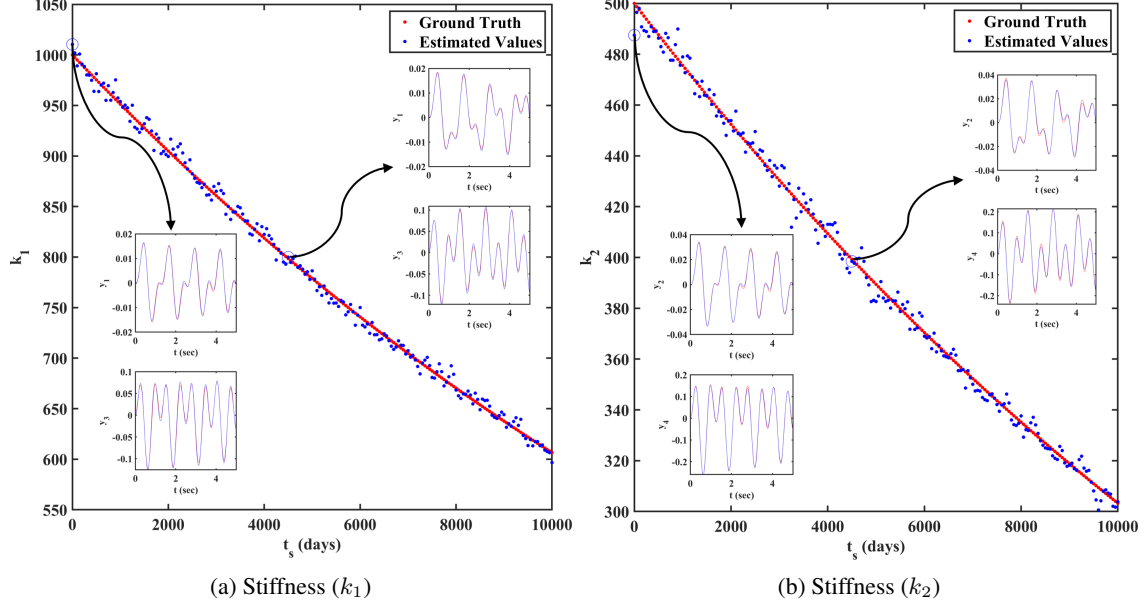


Figure 12: Estimated stiffness in slow-time-scale using the UKF algorithm for the 2DOF example. State estimations at selected time-steps are also shown. Good match between the ground truth and the filtered result is obtained. These data act as input to the Gaussian process (GP).

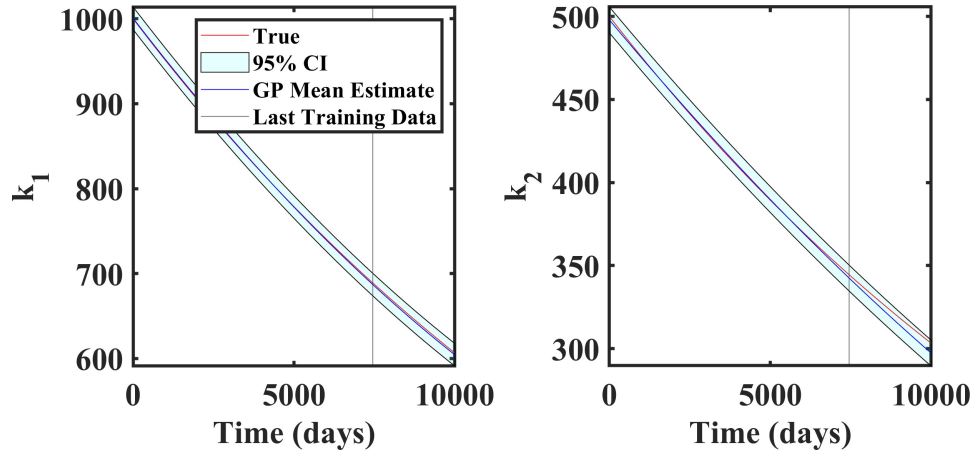


Figure 13: Results representing the performance of the proposed digital twin for the 2DOF system. The GP is trained using the data generated using UKF. Data upto the horizontal line is available to the GP. The digital twin performs well even when predicting system parameters at future time-steps.

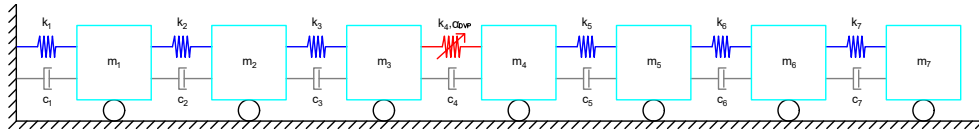


Figure 14: Schematic representation of the 7-DOF System with duffing Van-der Pol oscillator considered in example 2. The nonlinear DVP oscillator is attached with the fourth degree of freedom (shown in red).

Using Eq. (24), dispersion and drift matrices for 7-DOF system are identified as follows:

$$b_{ij} = \begin{cases} \frac{\sigma_i}{m_i}, & \text{for } i = 2j \text{ and } j = (1, 2, 3, 5, 6, 7) \\ \frac{\sigma_i}{m_i} y_{2j-1}, & \text{for } i = 2j \text{ and } j = 4 \\ 0, & \text{elsewhere} \end{cases} \quad (42)$$

Index i	Mass (Kg)	Stiffness Constant (N/m)	Damping Constant (Ns/m)	Force(N) $F_i = \lambda_i \sin(\omega_i t)$	Stochastic Noise Parameters
i = 1,2	$m_i = 20$	$k_i = 2000$	$c_i = 20$	$\lambda_i = 10, \omega_i = 10$	$s_i = 0.1$
i = 3,4,5,6	$m_i = 10$	$k_i = 1000$			
i = 7	$m_i = 5$	$k_i = 500$			
DVP Oscillator Constant, $\alpha_{DVP} = 100$					

Table 2: System Parameters – 7-DOF System – Data Simulation

$$\mathbf{a} = \begin{bmatrix} \frac{f_1}{m_1} - \frac{1}{m_1} (y_1 (k_1 + k_2) - c_2 y_4 - k_2 y_3 + y_2 (c_1 + c_2)) \\ y_4 \\ \frac{f_2}{m_2} + \frac{1}{m_2} (c_2 y_2 - y_3 (k_2 + k_3) + c_3 y_6 + k_2 y_1 + k_3 y_5 - y_4 (c_2 + c_3)) \\ y_6 \\ \frac{f_3}{m_3} - \frac{1}{m_3} (k_4 y_7 - c_4 y_8 - k_3 y_3 - c_3 y_4 + y_5 (k_3 - k_4) + \alpha_{DVP} (y_5 - y_7)^3 + y_6 (c_3 + c_4)) \\ y_8 \\ \frac{f_4}{m_4} + \frac{1}{m_4} (c_4 y_6 + c_5 y_{10} - k_4 y_5 + k_5 y_9 + y_7 (k_4 - k_5) + \alpha_{DVP} \{y_5 - y_7\}^3 - y_8 (c_4 + c_5)) \\ y_{10} \\ \frac{f_5}{m_5} + \frac{1}{m_5} (c_5 y_8 - y_9 (k_5 + k_6) + c_6 y_{12} + k_5 y_7 + k_6 y_{11} - y_{10} (c_5 + c_6)) \\ y_{12} \\ \frac{f_6}{m_6} + \frac{1}{m_6} (c_6 y_{10} - y_{11} (k_6 + k_7) + c_7 y_{14} + k_6 y_9 + k_7 y_{13} - y_{12} (c_6 + c_7)) \\ y_{14} \\ \frac{f_7}{m_7} + \frac{1}{m_7} (c_7 y_{12} - c_7 y_{14} + k_7 y_{11} - k_7 y_{13}) \end{bmatrix} \quad (43)$$

Similar to previous example data simulation is carried out using Taylor-1.5-Strong algorithm shown in Eq. (26) and filtering model is formed using EM equation shown in Eq. (27). For performing combined state parameter estimation state vector is modified to:

$$\mathbf{y} = [\mathbf{y}_{1:14}, \mathbf{k}_{1:7}]^T \quad (44)$$

Consequently \mathbf{a} and \mathbf{b} matrices are changed as: $\mathbf{a} = [\mathbf{a}_{state}^T, \mathbf{0}_{1 \times 6}]^T$ and $\mathbf{b} = [\mathbf{b}_{state}^T, \mathbf{0}_{7 \times 7}]^T$ where \mathbf{a}_{state} and \mathbf{b}_{state} are equal to \mathbf{a} and \mathbf{b} from Eq. (43) and Eq. (42) respectively. Note that although the value k_4 is a-priori known, we have still considered it into the state vector. It was observed that such a setup helps in regularizing the UKF estimates. Dynamic model function, $\mathbf{f}(\mathbf{y})$ is obtained using Eq. (29) and acceleration measurements are obtained using Eq. (32). Since for measurement, accelerations of all DOF are considered, measurement model for the UKF remains same as acceleration model and can be written as,

$$\mathbf{h}(\mathbf{y}) = \begin{bmatrix} -\frac{1}{m_1} (y_1 (k_1 + k_2) - c_2 y_4 - k_2 y_3 + y_2 (c_1 + c_2)) \\ \frac{1}{m_2} (c_2 y_2 - y_3 (k_2 + k_3) + c_3 y_6 + k_2 y_1 + k_3 y_5 - y_4 (c_2 + c_3)) \\ -\frac{1}{m_3} (k_4 y_7 - c_4 y_8 - k_3 y_3 - c_3 y_4 + y_5 (k_3 - k_4) + \alpha_{DVP} (y_5 - y_7)^3 + y_6 (c_3 + c_4)) \\ \frac{1}{m_4} (c_4 y_6 + c_5 y_{10} - k_4 y_5 + k_5 y_9 + y_7 (k_4 - k_5) + \alpha_{DVP} (y_5 - y_7)^3 - y_8 (c_4 + c_5)) \\ \frac{1}{m_5} (c_5 y_8 - y_9 (k_5 + k_6) + c_6 y_{12} + k_5 y_7 + k_6 y_{11} - y_{10} (c_5 + c_6)) \\ \frac{1}{m_6} (c_6 y_{10} - y_{11} (k_6 + k_7) + c_7 y_{14} + k_6 y_9 + k_7 y_{13} - y_{12} (c_6 + c_7)) \\ \frac{1}{m_7} (c_7 y_{12} - c_7 y_{14} + k_7 y_{11} - k_7 y_{13}) \end{bmatrix} \quad (45)$$

Process noise co-variance matrix \mathbf{Q} is obtained using the same process as discussed for 2-DOF system (refer Eq. (30)) and is written as,

$$\mathbf{q}_c = \sqrt{dt} \text{diag} \begin{bmatrix} 0 & \frac{\sigma_1}{m_1} & 0 & \frac{\sigma_2}{m_2} & 0 & \frac{\sigma_3}{m_3} & 0 & \frac{m_k^-(7)}{m_4} \frac{\sigma_4}{m_4} & 0 & \frac{\sigma_5}{m_5} & 0 & \frac{\sigma_6}{m_6} & 0 & \frac{\sigma_7}{m_7} & 0 & 0 & 0 & 0 & 0 & 0 \end{bmatrix} \quad (46)$$

$$\mathbf{Q} = \mathbf{q}_c \mathbf{q}_c^T$$

Where, $m_k^-(7)$ is the seventh element of UKF's predicted mean calculated from Eq. (11). The acceleration measurements and applied force are corrupted with a Gaussian noise having SNR values of 50 and 20 respectively. A comparison of the acceleration response obtained from data simulation and used in filtering is presented in Fig. 15.

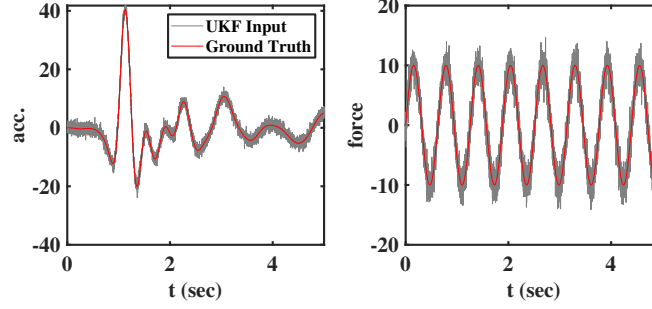


Figure 15: Sample Acceleration and deterministic component of the force for the 7-DOF problem. The stochasticity observed for the force is due to the noise present. Note that there is an additional stochastic component of force as shown in Eq. (27).

Similar to the previous example, we first examine the performance of the UKF algorithm. To that end, the acceleration vectors (noisy) shown in Fig. 16 is considered as the measurements. The state and parameter estimation results obtained using the UKF algorithm are shown in Fig. 17. It can be observed that the proposed approach yields highly accurate estimate of the state vectors. As for the parameter estimation, k_2 , k_3 and k_5 converge exactly towards their respective true values. As for k_1 , k_6 and k_7 , UKF yields an accuracy of around 95%. A summary of the estimated parameters in the slow time-scales is shown in Fig. 18 and Fig. 19. We observe that the estimates for new data points improve as our initial guess of system parameter improves (which for our case is the final parameters obtained from previous data points). Similar to Fig. 17, we observe that the estimates for stiffness k_2 , k_3 and k_5 are more accurate than those obtained for k_1 , k_6 and k_7 . These data is used for training the GP model. Fig. 20 shows the results obtained

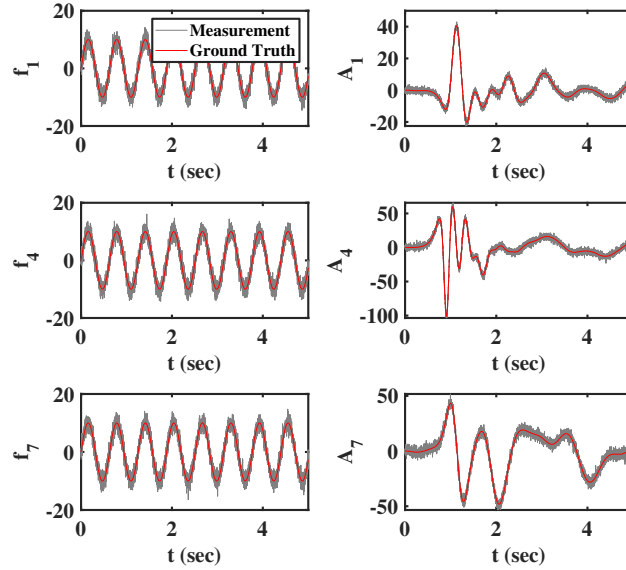


Figure 16: Deterministic component of force and acceleration vector corresponding to DOF 1, 4 and 7 used in UKF. The noisy acceleration vectors are provided as measurements to the UKF algorithm.

using the GP. The vertical line in Fig. 20 indicate the point until which data is available to the GP. For k_1 , k_2 , k_3 and k_5 , the results obtained using GP matches exactly with the true solution. For k_7 , the GP predicted results are found to diverge from the true solution. However, the divergence is observed approximately after 3.5 years from the last observation, which for all practical purpose is sufficient for condition based maintenance. For stiffness k_6 also, even though the filter estimates are less accurate at earlier time steps, the predicted results manage to give a good estimates of actual value which goes to show that if digital twin is given a regular stream of data, it has the capacity for self correction which in-turn helps better representation of the physical systems.

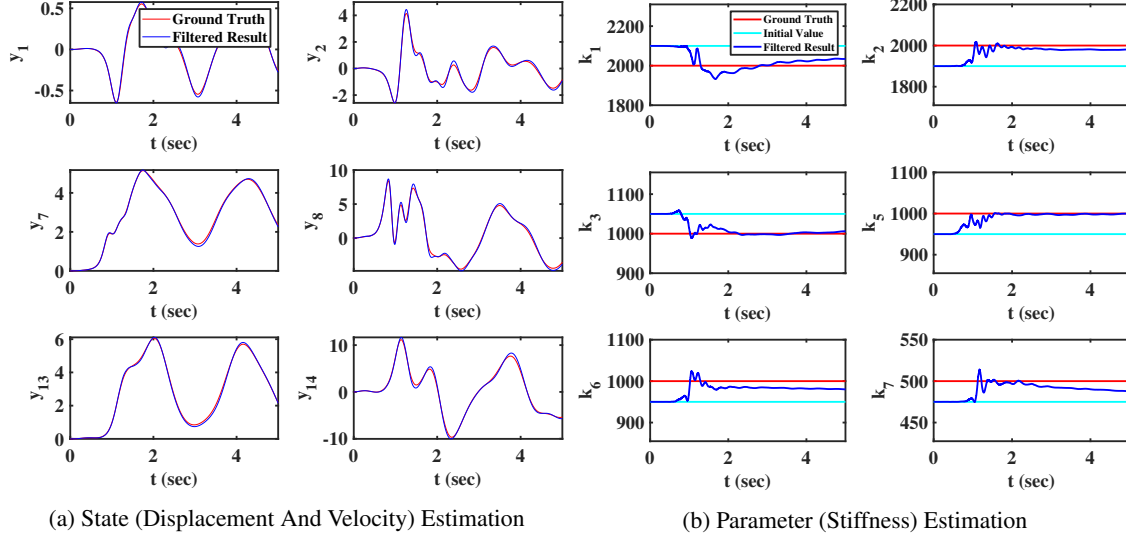
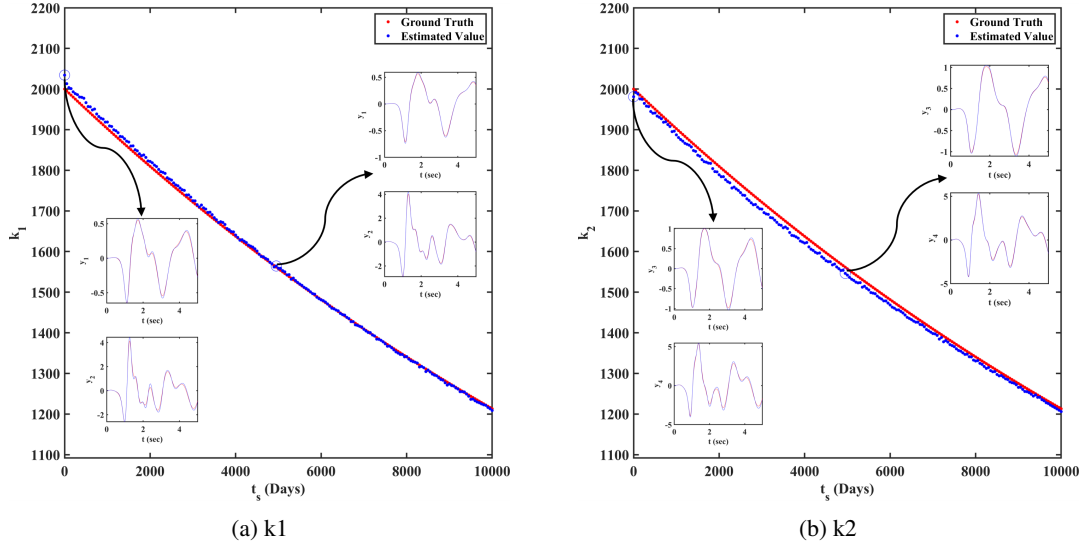


Figure 17: Combined state and parameter estimation results for the 7-DOF van der pol system.

Figure 18: Estimated stiffness (k_1 and k_2) in slow-time-scale using the UKF algorithm for the 7DOF example. State estimations at selected time-steps are also shown. Good match between the ground truth and the filtered result is obtained. These data act as input to the Gaussian process (GP).

7 Conclusions

The potential of digital twin in dynamical systems is immense; it can be used for health-monitoring, diagnosis, prognosis, active control and remaining useful life computation. However, practical adaptation of this technology has been slower than expected, particularly because of insufficient application-specific details. To address this issue, we propose a novel digital twin framework for stochastic nonlinear multi degree of freedom dynamical systems. The proposed digital twin has four components – (a) a physics-based nominal model (low-fidelity), (b) a Bayesian filtering algorithm (c) a supervised machine learning algorithm and (d) a high-fidelity model for predicting future responses. The physics-based nominal model combined with Bayesian filtering is used for combined parameter-state estimation, and the GP is used for learning the temporal evolution of the parameters. While the proposed framework can be used with any choice of Bayesian filtering and machine learning algorithm, the proposed approach uses unscented Kalman filter and Gaussian process in this paper.

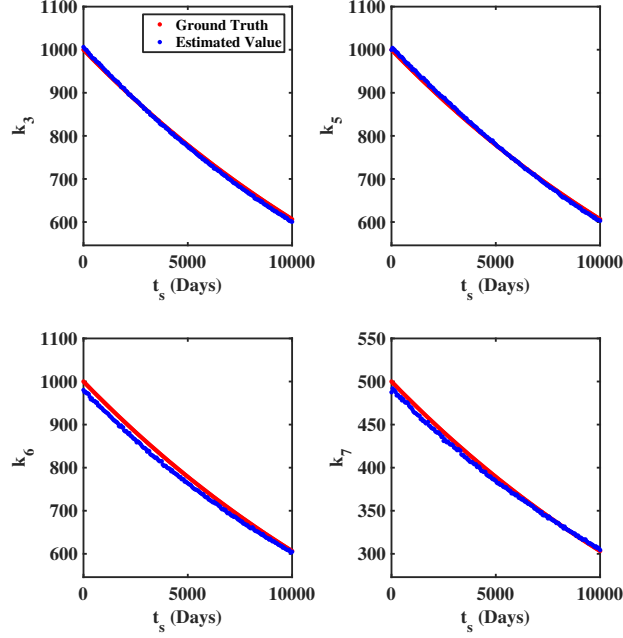


Figure 19: Estimated stiffness (k_3 , k_5 , k_6 and k_7) in slow-time-scale using the UKF algorithm for the 7DOF example. Good match between the ground truth and the filtered result is obtained. These data act as input to the Gaussian process (GP).

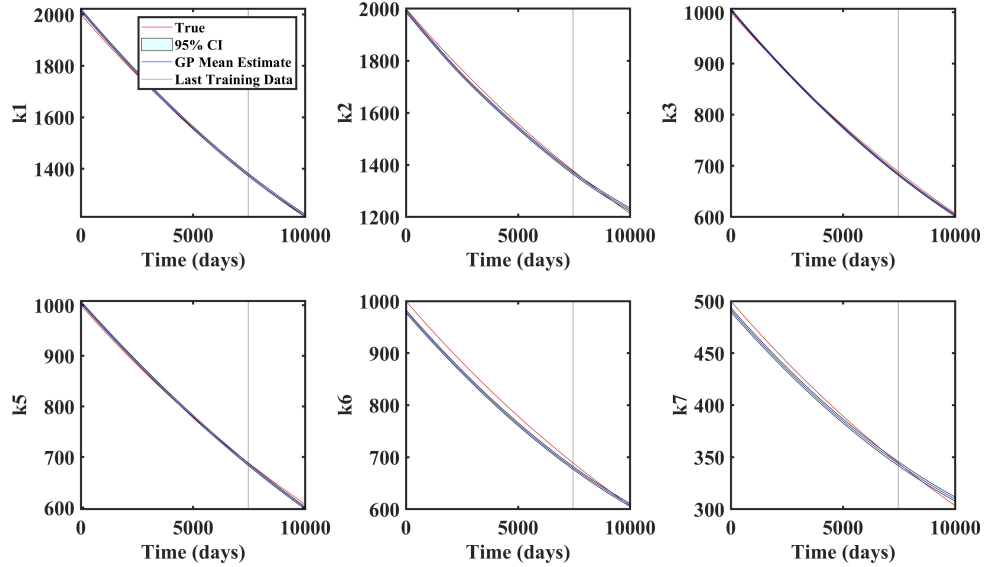


Figure 20: Results representing the performance of the proposed digital twin for the 7DOF system. The GP is trained using the data generated using UKF. Data upto the horizontal line is available to the GP. The digital twin performs well even when predicting system parameters at future time-steps.

Applicability of the proposed digital twin is illustrated with two stochastic nonlinear MDOF systems. For both examples, we have assumed availability of acceleration measurements and the stochasticity is present in the applied force. In order to simulate a realistic scenario, a high-fidelity model (Taylor 1.5 strong) is used for data generation and a low-fidelity model (Euler Maruyama) is used for filtering. The synthetic measurement data generated are corrupted with white Gaussian noise. Cases pertaining to partial measurements (measurement at only selected degrees of freedom) and complete measurement (measurements at all degrees of freedom) are shown. For all the cases, the proposed digital twin is found to yield highly accurate results with accuracy of 95% and above, indicating its possible application to other realistic systems.

Acknowledgements

AG and BH gratefully acknowledges the financial support received from Science and Engineering Research Board (SERB), Department of Science and Technology (DST), Government of India, (under the project no. IMP/2019/000276). SC acknowledges the financial support received from I-Hub foundation for Cobotics (IHFC) through seed funding.

References

- [1] Vinicius Souza, Robson Cruz, Waldir Silva, Sidney Lins, and Vicente Lucena. A digital twin architecture based on the industrial internet of things technologies. In *2019 IEEE International Conference on Consumer Electronics (ICCE)*, pages 1–2. IEEE, 2019.
- [2] Athena Stassopoulou, Maria Petrou, and Josef Kittler. Application of a bayesian network in a gis based decision making system. *International Journal of Geographical Information Science*, 12(1):23–46, 1998.
- [3] Xiao-Sheng Si, Wenbin Wang, Chang-Hua Hu, and Dong-Hua Zhou. Remaining useful life estimation—a review on the statistical data driven approaches. *European journal of operational research*, 213(1):1–14, 2011.
- [4] Jonathan S Tan and Mark A Kramer. A general framework for preventive maintenance optimization in chemical process operations. *Computers & Chemical Engineering*, 21(12):1451–1469, 1997.
- [5] Jinjiang Wang, Lunkuan Ye, Robert X Gao, Chen Li, and Laibin Zhang. Digital twin for rotating machinery fault diagnosis in smart manufacturing. *International Journal of Production Research*, 57(12):3920–3934, 2019.
- [6] Wihan Booyse, Daniel N Wilke, and Stephan Heyns. Deep digital twins for detection, diagnostics and prognostics. *Mechanical Systems and Signal Processing*, 140:106612, 2020.
- [7] Yuqian Lu, Chao Liu, I Kevin, Kai Wang, Huiyue Huang, and Xun Xu. Digital twin-driven smart manufacturing: Connotation, reference model, applications and research issues. *Robotics and Computer-Integrated Manufacturing*, 61:101837, 2020.
- [8] Tarasankar Debroy, Wei Zhang, J Turner, and Sudarsanam Suresh Babu. Building digital twins of 3d printing machines. *Scripta Materialia*, 135:119–124, 2017.
- [9] Chenzhao Li, Sankaran Mahadevan, You Ling, Sergio Choe, and Liping Wang. Dynamic bayesian network for aircraft wing health monitoring digital twin. *Aiaa Journal*, 55(3):930–941, 2017.
- [10] Michael G Kapteyn, David J Knezevic, and Karen Willcox. Toward predictive digital twins via component-based reduced-order models and interpretable machine learning. In *AIAA Scitech 2020 Forum*, page 0418, 2020.
- [11] Sondipon Adhikari and Subhamoy Bhattacharya. Dynamic analysis of wind turbine towers on flexible foundations. *Shock and vibration*, 19(1):37–56, 2012.
- [12] R Ganguli and S Adhikari. The digital twin of discrete dynamic systems: Initial approaches and future challenges. *Applied Mathematical Modelling*, 77:1110–1128, 2020.
- [13] Souvik Chakraborty, Sondipon Adhikari, and Ranjan Ganguli. The role of surrogate models in the development of digital twins of dynamic systems. *Applied Mathematical Modelling*, 90:662–681, 2021.
- [14] Christopher Williams and Carl Rasmussen. Gaussian processes for regression. *Advances in neural information processing systems*, 8:514–520, 1995.
- [15] Rajdip Nayek, Souvik Chakraborty, and Sriram Narasimhan. A gaussian process latent force model for joint input-state estimation in linear structural systems. *Mechanical Systems and Signal Processing*, 128:497–530, 2019.
- [16] Souvik Chakraborty and Rajib Chowdhury. Graph-theoretic-approach-assisted gaussian process for nonlinear stochastic dynamic analysis under generalized loading. *Journal of Engineering Mechanics*, 145(12):04019105, 2019.
- [17] Tapas Tripura, Ankush Gogoi, and Budhaditya Hazra. An ito–taylor weak 3.0 method for stochastic dynamics of nonlinear systems. *Applied Mathematical Modelling*, 86:115–141, 2020.
- [18] Basuraj Bhowmik, Tapas Tripura, Budhaditya Hazra, and Vikram Pakrashi. First-order eigen-perturbation techniques for real-time damage detection of vibrating systems: Theory and applications. *Applied Mechanics Reviews*, 71(6), 2019.
- [19] Souvik Chakraborty and Sondipon Adhikari. Machine learning based digital twin for dynamical systems with multiple time-scales. *Computers & Structures*, 243:106410, 2021.

- [20] TG Ritto and FA Rochinha. Digital twin, physics-based model, and machine learning applied to damage detection in structures. *Mechanical Systems and Signal Processing*, 155:107614, 2021.
- [21] Simo Särkkä. *Bayesian filtering and smoothing*, volume 3. Cambridge University Press, 2013.
- [22] Zhe Chen et al. Bayesian filtering: From kalman filters to particle filters, and beyond. *Statistics*, 182(1):1–69, 2003.
- [23] Ka-Veng Yuen and Sin-Chi Kuok. Bayesian methods for updating dynamic models. *Applied Mechanics Reviews*, 64(1), 2011.
- [24] Somdatta Goswami, Cosmin Anitescu, Souvik Chakraborty, and Timon Rabczuk. Transfer learning enhanced physics informed neural network for phase-field modeling of fracture. *Theoretical and Applied Fracture Mechanics*, 106:102447, 2020.
- [25] Souvik Chakraborty. Transfer learning based multi-fidelity physics informed deep neural network. *Journal of Computational Physics*, 426:109942, 2021.
- [26] Souvik Chakraborty and Rajib Chowdhury. Modelling uncertainty in incompressible flow simulation using galerkin based generalized anova. *Computer Physics Communications*, 208:73–91, 2016.
- [27] Souvik Chakraborty and Rajib Chowdhury. Polynomial correlated function expansion. In *Modeling and simulation techniques in structural engineering*, pages 348–373. IGI global, 2017.
- [28] Ilias Bilonis and Nicholas Zabarar. Multi-output local gaussian process regression: Applications to uncertainty quantification. *Journal of Computational Physics*, 231(17):5718–5746, 2012.
- [29] Ilias Bilonis, Nicholas Zabarar, Bledar A Konomi, and Guang Lin. Multi-output separable gaussian process: Towards an efficient, fully bayesian paradigm for uncertainty quantification. *Journal of Computational Physics*, 241:212–239, 2013.
- [30] Vasilis K Dertimanis, EN Chatzi, S Eftekhar Azam, and Costas Papadimitriou. Input-state-parameter estimation of structural systems from limited output information. *Mechanical Systems and Signal Processing*, 126:711–746, 2019.
- [31] Jianye Ching, James L Beck, and Keith A Porter. Bayesian state and parameter estimation of uncertain dynamical systems. *Probabilistic engineering mechanics*, 21(1):81–96, 2006.
- [32] Patrick T Brewick, Sami F Masri, Anastasios G Chassiakos, and Elias B Kosmatopoulos. A probabilistic study of the robustness of an adaptive neural estimation method for hysteretic internal forces in nonlinear mdof systems. *Probabilistic Engineering Mechanics*, 45:140–156, 2016.
- [33] Nilanjan Saha and D Roy. Extended kalman filters using explicit and derivative-free local linearizations. *Applied Mathematical Modelling*, 33(6):2545–2563, 2009.
- [34] Eric A Wan and Rudolph Van Der Merwe. The unscented kalman filter for nonlinear estimation. In *Proceedings of the IEEE 2000 Adaptive Systems for Signal Processing, Communications, and Control Symposium (Cat. No. 00EX373)*, pages 153–158. Ieee, 2000.
- [35] Greg Welch, Gary Bishop, et al. An introduction to the kalman filter, 1995.
- [36] Yash Kumar, Pranav Bahl, and Souvik Chakraborty. State estimation with limited sensors—a deep learning based approach. *arXiv preprint arXiv:2101.11513*, 2021.
- [37] Souvik Chakraborty. Simulation free reliability analysis: A physics-informed deep learning based approach. *arXiv preprint arXiv:2005.01302*, 2020.
- [38] Eyke Hüllermeier and Willem Waegeman. Aleatoric and epistemic uncertainty in machine learning: An introduction to concepts and methods. *Machine Learning*, pages 1–50, 2021.
- [39] Carl Edward Rasmussen. Gaussian processes in machine learning. In *Summer school on machine learning*, pages 63–71. Springer, 2003.
- [40] Debasish Roy and G Visweswara Rao. *Stochastic dynamics, filtering and optimization*. Cambridge University Press, 2017.
- [41] Armand Wirgin. The inverse crime. *arXiv preprint math-ph/0401050*, 2004.
- [42] Sourav Das, Souvik Chakraborty, Yangyang Chen, and Solomon Tesfamariam. Robust design optimization for sma based nonlinear energy sink with negative stiffness and friction. *Soil Dynamics and Earthquake Engineering*, 140:106466, 2021.
- [43] Dongxing Cao, Xiangying Guo, and Wenhua Hu. A novel low-frequency broadband piezoelectric energy harvester combined with a negative stiffness vibration isolator. *Journal of Intelligent Material Systems and Structures*, 30(7):1105–1114, 2019.